the F band or annealing of the volume expansion. There is, to be sure, growth and annealing of aggregate centers, but these are in much too small a concentration to account for the energy. Thus, most of the energy must come either from electronic transitions not showing up in our optical measurements, or from atomic rearrangements which do not change the volume. The former might be electrons and holes in shallow traps annihilating, and the latter might be the annihilation of interstitials at vacancy clusters. An electronic mechanism seems to offer more possibility for accounting for the large energy.

In the temperature region 170–290°C, all known coloring bleaches, most of the stored energy is released, and volume annealing begins and is nearly completed. The data indicate that the F- and M-band bleaching occur at lower temperatures than the volume annealing. We suggest, then, that the stored-energy spectrum at these temperatures consists of at least two unresolved peaks. The case of the calcium-doped specimen seems to support this, since its optical bleaching occurs at a much lower temperature. It might be significant that the temperature of maximum energy-release rate is higher for the higher colorations.

Between 290 and 400°C there are no more optical effects, but there is still considerable stored-energy release and volume annealing. Since the stored energy here is proportional to the *initial* M-center concentration, a plausible model is that the M-center divacancies are migrating to surfaces. The energy of 1.5 eV per M center, Fig. 11, seems reasonable.

In the calcium-doped specimen, all of the bleaching, and most of the stored-energy release occurs in the lowest of our three temperature ranges. One might be inclined to ascribe the stored-energy release under the 135°C peak for the pure specimens to impurities similar to calcium. We think that the evidence is against this. The pure specimens show no bleaching to correspond to that peak, even though it has appreciable energy. Note also that the stored energy per F center in the doped crystal is about the same as that of the pure crystals, in spite of the very different annealing behavior. Perhaps the calcium acts as a kind of catalyst that enables the F centers to bleach at lower temperatures without changing the net energy release.

It might be fruitful to study stored energy in other alkali halides. With luck, one might find a compound where the various processes occur at more widely separated temperatures, thus giving more peaks and enabling the assignment of energies to processes.

PHYSICAL REVIEW VOLUME 181, NUMBER 3 15 MAY 1969

Refractive Indices of the Condensed Inert Gases

A. C. SINNOCK*
Department of Applied Physics, Brighton College of Technology, Brighton, Sussex, England
AND
B. L. SMITH
School of Mathematical and Physical Sciences, University of Sussex, Falmer, Sussex, England
(Received 16 July 1968)

The refractive indices of condensed argon, krypton, and xenon have been measured for wavelengths between 3612 and 6439 Å by the spectroscopic method of minimum deviation. The Lorentz-Lorenz functions f_{LL} are found to remain constant to within about 3% over the entire range studied, with a small decrease (~1%) on freezing. At higher solid densities, the f_{LL} functions decrease with increasing density at an accelerating rate. This behavior is in moderate agreement only with theoretical predictions based on the tight-binding exciton model.

I. INTRODUCTION

IT has recently been proposed[1–3] that the low-frequency dielectric properties of the solidified inert gases could be described in terms of a tight-binding exciton model. Existing experimental data[4–6] are not sufficiently extensive to provide an adequate test of theories based on such a model. We have therefore measured the refractive indices (n) of solid argon, krypton, and xenon[7] over a wide range of temperature and at wavelengths in the region 3612–6439 Å. In addition, we report the results of measurements on the liquids in equilibrium with their vapors at temperatures close to the triple points.

According to the Lorentz local-field model, the

* Work carried out in the School of Mathematical and Physical Sciences, University of Sussex.
[1] T. H. Keil, J. Chem. Phys. **46**, 4404 (1967).
[2] S. Doniach and R. Huggins, Phil. Mag. **12**, 393 (1965).
[3] R. Mazo, J. Am. Chem. Soc. **86**, 3470 (1964).
[4] G. O. Jones and B. L. Smith, Phil. Mag. **5**, 355 (1960).
[5] A. J. Eatwell and G. O. Jones, Phil. Mag. **10**, 1059 (1964).
[6] B. L. Smith and C. J. Pings, J. Chem. Phys. **38**, 825 (1963).
[7] Preliminary measurements have been reported by A. C. Sinnock and B. L. Smith, Phys. Letters **24A**, 387 (1967); **28A**, 22 (1968).

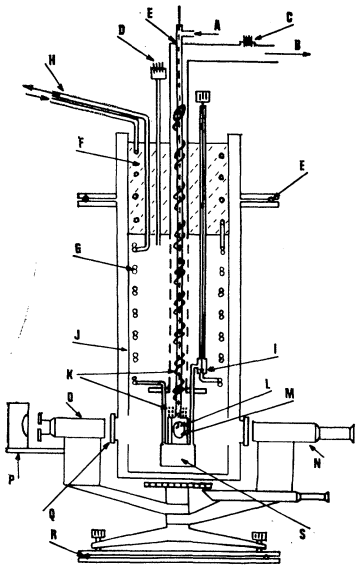

FIG. 1. Apparatus used in present investigation. (A) Gas sample inlet, (B) outlet to vacuum system, (C) heater lead in, (D) thermocouple lead in, (E) o-ring seals, (F) liquid-nitrogen reservoir, (G) heat exchangers, (H) hydrogen inlet and outlet tubes, (I) throttling needle valve, (J) radiation shield at 77°K, (K) stem and prism heaters, (L) thermocouple mounted inside prism cell, (M) prism cell with sapphire windows, (N) telescope and cross wires, (O) collimator and slit, (P) spectral lamp, (Q) vacuum jacket windows, (R) co-axial turntable, and (S) liquid-hydrogen can.

dielectric constant ϵ of a homogeneous nonpolar medium is related to the polarizability α and the density ρ by the Lorentz-Lorenz function

$$\frac{(n^2-1)}{(n^2+2)}\frac{1}{\rho}=\frac{(\epsilon-1)}{(\epsilon+2)}\frac{1}{\rho}=\frac{4\pi N_0\alpha}{3M}=f_{\mathrm{LL}}, \qquad (1)$$

where M is the molecular weight and N_0 is Avogadro's number. Measurements at low and moderate densities, for example, on argon[8] and carbon dioxide,[9] show that although f_{LL} is indeed nearly independent of density as implied by Eq. (1), small but significant deviations do occur. Starting at low density, f_{LL} increases slowly with density, passes through a maximum at about 200 amagats, and then decreases rather more rapidly. This behavior is moderately well understood and has been described in terms of the effect of statistical fluctuations on the induced dipole moment.[10,11] Quadrupole-quadrupole and higher-order interactions contribute slightly to the increase in f_{LL},[12,13] and at higher densities (>500 amagats), α changes significantly from the free-atom value because individual molecules are "caged" by their neighbors.[14] Since the solidified inert gases have the symmetry required by the Lorentz model and the effects of overlap are probably small,[15] their dielectric behavior should be described adequately by Eq. (1), provided that α is suitably modified to take account of density.

Since these substances are nonpolar, $\epsilon=n^2$, where n is the refractive index. The inert gases condense to form colorless liquids and freeze under suitable conditions to form transparent solids. Hence it is possible to determine the refractive index rather than the dielectric constant. Optical measurements are generally more simple to make than electrical ones and yield accurate results with fewer corrections.

II. PRINCIPLE OF METHOD

The refractive index was measured by the spectroscopic method of minimum deviation.[16] In this method a prism-shaped specimen is confined in an optical cell contained in a cryostat and located at the axis of rotation of a spectrometer mounted outside the cryostat on a coaxial turntable. The refractive index n is found from the angle of minimum deviation D and the angle of the prism A by means of the relation

$$n=\sin\tfrac{1}{2}(A+D)/\sin\tfrac{1}{2}A. \qquad (2)$$

Measurements were made at various wavelengths using spectral lines from a mercury-cadmium-zinc lamp. A large number of observations were made for the 5461 Å line and somewhat fewer at other wavelengths in the range 4358–6439 Å. In addition, the spectrum was recorded photographically, thus allowing angles of minumum deviation corresponding to wavelengths in the range 3612–4358 Å to be deduced.

III. EXPERIMENTAL

The arrangement of the cell, cryostat, and spectrometer is shown in Fig. 1. It is a modified version of apparatus previously described by Smith.[17] The solid is condensed in a hollow stainless-steel prism (M) with sapphire windows, mounted upon the hydrogen state of a miniature hydrogen liquefier.[18] The sapphires were cut with the C axis perpendicular to the faces and polished to 0.00005 cm flatness and 30 sec of arc parallelism. They were sealed to the block with A.T.I. Araldite epoxy resin, obtained from CIBA (A.R.L.) Ltd., Cambridge, England, and were tested prior to the experiment by thermal cycling.

The prism angle was determined by filling the prism with water and measuring the angle of minimum deviation as a function of temperature. Experimental data

[8] A. Michels, C. A. ten Seldam, and S. D. J. Overdijk, Physica **17**, 781 (1951).
[9] A. Michels and L. Kleerckoper, Physica **6**, 586 (1939).
[10] J. Yvon, *Recherche sur la Theories Cinetique des Liquides* (Herman et Cie., Paris, 1937).
[11] J. G. Kirkwood, J. Chem. Phys. **4**, 592 (1936).
[12] L. Jansen and P. Mazur, Physica **21**, 193 (1955).
[13] A. D. Buckingham, Trans. Faraday Soc. **52**, 1035 (1956).
[14] C. A. ten Seldam and S. R. de Groot, Physica **18**, 910 (1952).
[15] R. F. Guertin and F. Stern, Phys. Rev. **134**, 427 (1964).
[16] E. C. C. Baly, *Spectroscopy* (Longmans Green and Co., Inc., New York, 1929), p. 48.
[17] B. L. Smith, Rev. Sci. Instr. **34**, 19 (1963).
[18] B. Yates and F. E. Hoare, Cryogenics **2**, 84 (1961).

for the refractive index of water by Rosen[19] and by Tilton and Taylor[20] were used to deduce the effective prism angle and to investigate the possibility of prism distortion under pressure. The angle was found to be 45°38′46″, and no significant temperature or pressure variation was found. Since the cryostat jacket was under continuous evaluation during the experiment, the measurements yield absolute values of the refractive index.

The temperature of the sample was established from readings of calibrated copper-constantan thermocouples mounted at the top and bottom of the prism block and also one located inside the cell (L), in the center of the specimen. Temperatures were measured to ± 0.2 μV (± 0.01°K at 80°K), but because of the low thermal conductivity of the solid specimens, the absolute accuracy is estimated to be only ± 0.1°K.

Solid samples were formed by slowly admitting the gas to the cell while the base of the prism block was maintained at a predetermined temperature. It was found possible to grow specimens free of visual defects[21] at temperatures near the triple point from either the liquid or the vapor phase, provided that the sample was formed very slowly and care was taken to avoid vapor snakes.[22] During formation, the stem heater (K) was switched on to avoid condensation in the entry tube, and the heater at the top of the prism operated in order to maintain a temperature gradient in the specimen. When the cell was half-filled, the heater currents were slowly reduced over a period of about 30 min, and the specimen was then allowed to anneal for a further period.

Solid samples varied considerably in quality. At temperatures below about 0.5 of the triple point, it proved extremely difficult to obtain specimens that were sufficiently transparent for reliable optical measurements to be made. At temperatures close to the triple point, defects could be annealed out over a period of a few hours, whereas at lower temperatures they appeared to be frozen into the sample. Observations made on a specimen of solid argon near the triple point over a period of several hours showed a change in the angle of minimum deviation of about 5′. Similar annealing effects have been reported by Lawrence and Neale[23] and by Lefkowitz *et al.*[24] Liquid samples were formed by condensing the gas directly into the prism at the appropriate temperature and allowing sufficient time for thermal equilibrium to be reached.

Measurements of minimum deviation were made optically at 6439, 5780, 5461, 5086, 4806, 4700, and 4358 Å, although it was not always possible to distinguish all the lines for argon and krypton because of the smaller dispersion relative to xenon. In addition, photographs were taken of the refracted spectrum, with the telescope fixed in the minimum deviation position for the 5461 Å line. The spacings between the lines on the negative were measured using a recording microdensitometer and used to obtain angles of minimum deviation corresponding to 4063, 3650, and 3612 Å.

Angles A and D were determined to within $\pm 30''$ of arc absolute. The maximum error in n is estimated to be about $\pm 0.1\%$. The relative error of measurements at the same temperature but at different wavelengths is considerably smaller.

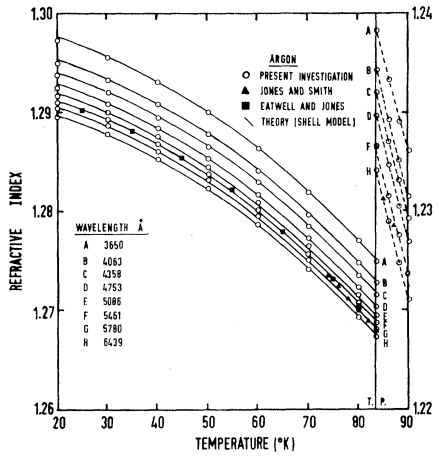

FIG. 2. Refractive indices of liquid and solid argon. The continuous lines correspond to Eq. (12) with values $\omega_0 = 11.725$ eV, $\omega_p^2 = 31.69$ eV^2, $U_0^3(\mathrm{TP}) = 7.99$ eV^2, $\chi_1 = 0.2811$, and $B_5 = 12$. To avoid confusion, not all data points are included in the figure.

IV. RESULTS

A. Liquid and Solid Argon

The results for the refractive indices of liquid and solid argon are compared with those of previous investigations in Fig. 2. To avoid confusion the figure only includes points from other data that correspond to 5461 Å. In the low-temperature liquid region the only direct measurements available are by Jones and Smith.[4] These agree with the present value at the triple point ($n_{\mathrm{TP}} = 1.2334$) to within 0.0002 ($\sim 0.02\%$). Refractive-index measurements due to Michels and Botzen,[25] and Teague and Pings[26] may be extrapolated to the triple point from low-density data extending to $0.90\rho_{\mathrm{TP}}$ and $0.96\rho_{\mathrm{TP}}$, respectively. These, when adjusted to 5461 Å, give values of 1.2316 and 1.2334. However, Michels and Botzen carried out their measurements at 298°K and thus their low value might indicate a slight tem-

[19] J. S. Rosen, J. Opt. Soc. Am. **37**, 832 (1947).
[20] L. W. Tilton and J. K. Taylor, J. Res. Natl. Bur. Std. (U. S.) **20**, 419 (1938).
[21] B. L. Smith and J. A. Chapman, Phil. Mag. **15**, 739 (1967).
[22] M. K. Phibbs and H. I. Schiff, J. Chem. Phys. **17**, 843 (1949).
[23] D. J. Lawrence and F. E. Neale, Proc. Phys. Soc. (London) **85**, 1251 (1965).
[24] I. Lefkowitz, K. Kramer, M. A. Shields, and G. L. Pollack, J. Appl. Phys. **38**, 4867 (1967).
[25] A. Michels and A. Botzen, Physica **6**, 586 (1949).
[26] R. K. Teague and C. J. Pings, J. Chem. Phys. **48**, 4973 (1968).

TABLE I. Smoothed values of refractive index, density, and f_{LL} for liquid and solid argon as a function of wavelength (Å). f_{LL} is computed for 5461 Å, using density values for the solid that assume negligible vacancy concentration (see text).

T °K	Wavelength (Å) 6439	5780	5461	5086	4753	4358	4063[b]	3650[b]	3612[b]	ρ[a] (10^{-2} mole/cm^3)	LL (cm^3/mole)
Solid											
20	1.2895	1.2903	1.2910	1.2918	1.2926	1.2938	1.2950	1.2972	1.2975	4.416	4.117
30	1.2879	1.2887	1.2894	1.2901	1.2909	1.2921	1.2934	1.2956	1.2959	4.385	4.124
40	1.2854	1.2862	1.2869	1.2876	1.2885	1.2896	1.2909	1.2931	1.2934	4.343	4.132
50	1.2822	1.2831	1.2838	1.2845	1.2853	1.2865	1.2878	1.2900	1.2903	4.293	4.138
60	1.2786	1.2795	1.2801	1.2809	1.2817	1.2829	1.2841	1.2863	1.2866	4.235	4.144
70	1.2742	1.2751	1.2757	1.2765	1.2773	1.2785	1.2797	1.2820	1.2822	4.170	4.148
80	1.2693	1.2702	1.2708	1.2716	1.2724	1.2736	1.2748	1.2771	1.2773	4.093	4.156
83.81	1.2673	1.2681	1.2688	1.2695	1.2704	1.2716	1.2728	1.2750	1.2753	4.061	4.160
Liquid											
83.81	1.2321	1.2328	1.2334	1.2341	1.2349	1.2361	1.2372	1.2392	1.2395	3.549	4.1707
86	1.2295	1.2303	1.2308	1.2316	1.2324	1.2336	1.2347	1.2367	1.2370	3.513	4.1704
88	1.2274	1.2282	1.2287	1.2295	1.2303	1.2315	1.2326	1.2346	1.2349	3.481	4.1722
90	1.2256	1.2264	1.2269	1.2277	1.2285	1.2297	1.2308	1.2331	1.2326	3.449	4.1794

[a] Solid densities, Ref. 29; liquid densities, D. C. Piercey, M.Sc. thesis, University of London, 1956, (unpublished); B. L. Smith, Phil. Mag. 6, 939 (1961); J. T. Mullhaupt and F. S. DiPaolo (private communication).
[b] Vaules deduced from photographs.

perature dependence of the refractive index.[27] The dielectric constant determination by Amey and Cole,[28] converted to 5461 Å by graphical means, is equivalent to 1.2336, and thus is also in good agreement.

The results for solid argon (Fig. 2) are also consistent with previous data. The wavelength dependences of the refractive index reported by Eatwell and Jones[5] and by Jones and Smith[4] agree within experimental error with those obtained in the present investigation, but are less accurate and extend over smaller wavelength ranges. The pressure measurements due to Smith and Pings,[6] adjusted to equilibrium vapor pressure and 5461 Å, and the dielectric constant measurement of Amey and Cole converted to 5461 Å, are both slightly higher (~0.2%) than the present value at the triple point. Since the errors associated with the *temperature* dependence of the refractive index in the measurements of Eatwell and Jones, Jones and Smith, and the present work are comparable, all these data have been used to establish the smoothed values of refractive index and f_{LL} given in Table I. Much more weight, however, has been given to the *wavelength* dependence of n obtained in the present investigation since it has been established with relatively greater certainty.

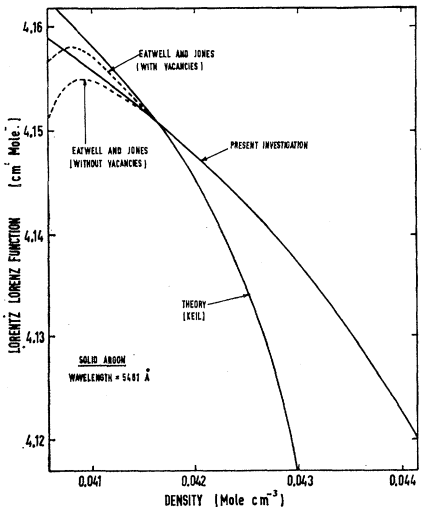

FIG. 3. Variation of f_{LL} with temperature for solid argon (5461 Å). The effect of an 0.13% vacancy concentration on the results of Eatwell and Jones is to reduce but not remove the positive slope near the triple point. The theoretical curve is based on the tight-binding calculation by Keil (see Sec. VI).

The function f_{LL} for the liquid decreases with increasing density by about 0.2% over the range studied, which is approximately the amount to be expected by comparison with the behavior of the compressed gas at lower densities.[8] The variation of f_{LL} with density for solid argon close to the triple point is in some doubt. The results of Eatwell and Jones (Fig. 3), and of Jones and Smith, suggest an initial increase with increasing density which has not been found in the present investigation, even though the refractive-index values agree within experimental error. This is because near the triple point the rates of variation of $(n^2-1)/(n^2+2)$ and ρ are of the same order of magnitude but of opposite sign. Thus, small uncertainties in the density may readily lead to a change in slope. It is well established that the defect concentration, and hence the density, changes fairly rapidly with time as annealing takes place.[21,29] Thus, if the density and refractive index data are not matched, in the sense that they relate to specimens of similar "metallurgical" history, considerable variation in f_{LL} will result.

It should be noted that the data shown in Fig. 3

[27] J. A. Chapman, P. C. Finnimore, and B. L. Smith, Phys. Rev. Letters 21, 1306 (1968).
[28] R. L. Amey and R. H. Cole, J. Chem. Phys. 40, 146 (1964).
[29] O. G. Peterson, D. N. Batchelder, and R. O. Simmons, Phys. Rev. 150, 703 (1966).

TABLE II. Smoothed values of refractive index, density f_{LL} for liquid and solid krypton as a function of wavelength (Å). f_{LL} is computed for 5461 Å, using density values for the solid that assume negligible vacancy concentration (see text).

T °K	Wavelength (Å) 6439	5780	5461	5086	4753	4358	4063[b]	3631[b]	ρ[a] (10^{-2} mole/cm³)	LL cm³/mole
Solid										
67	1.3648	1.3664	1.3674	1.3688	1.3704	1.3727	1.3749	1.3787	3.542[5]	6.344
75	1.3622	1.3638	1.3648	1.3662	1.3678	1.3701	1.3723	1.3761	3.511[5]	6.360
85	1.3587	1.3602	1.3612	1.3627	1.3642	1.3666	1.3688	1.3726	3.471[4]	6.377
95	1.3547	1.3562	1.3572	1.3587	1.3603	1.3626	1.3648	1.3686	3.429	6.392
105	1.3498	1.3514	1.3524	1.3538	1.3554	1.3578	1.3600	1.3638	3.383	6.400
115.95	1.3436	1.3451	1.3462	1.3476	1.3492	1.3515	1.3537	1.3576	3.330	6.398
Liquid										
115.95	1.3011	1.3024	1.3032	1.3042	1.3056	1.3074	1.3090	1.3120	2.926	6.453
118	1.2986	1.2999	1.3008	1.3017	1.3031	1.3049	1.3065	1.3095	2.906	6.449
122	1.2939	1.2952	1.2960	1.2970	1.2984	1.3002	1.3018	1.3048	2.868	6.441
126	1.2893	1.2906	1.2915	1.2924	1.2938	1.2957	1.2973	1.3003	2.829	6.438

[a] Solid densities, B. F. Figgins and B. L. Smith, Phil. Mag. **5**, 186 (1960); liquid densities, D. C. Piercey, M.Sc. thesis, University of London, (1956) (unpublished); E. Mathias, C. A. Crommelin, and J. J. Meihuizen, Physica **4**, 1200 (1937).
[b] Values deduced from photographs.

have been computed using density values derived from x-ray lattice-parameter measurements by Peterson *et al.*[29] for the perfect crystal. Smith and Chapman[21] have shown that at the triple point the equilibrium vacancy concentration in solid argon is $\mathbf{n/N} \leqslant 0.13\%$. If one assumes that in the crystals used by Eatwell and Jones the concentration lies close to the upper limit and that the temperature variation is given by $\mathbf{n/N} = \exp(-g_v/kT)$, where the free energy of a vacancy[30,31] $g_v \approx 1100$ cal mole^{-1}, a revised density and hence f_{LL} may be obtained. This is shown by the dashed line in Fig. 3.

At higher densities, corresponding to temperatures below ~78°K, the function f_{LL} decreases monotonically with increasing density, and it is believed that this behavior represents the significant result of the present investigation.

The gas used was supplied by the British Oxygen Company and was stated to be at least 99.9995% argon, the principal impurities being nitrogen, oxygen, and hydrogen.

B. Liquid and Solid Krypton

The refractive-index results for liquid and solid krypton are shown in Fig. 4. The only other data available for comparison are refractive-index measurements by Smith[32] for the solid, and dielectric constant determinations by Amey and Cole for the liquid and solid. Smith found that f_{LL} for solid krypton increased with increasing density over the range 71–109°K. This is inconsistent with the observations of the present investigation and is thought to be due to the relatively impure gas used in the earlier determination. The sample contained up to 0.5% xenon, and it is now known[33] that small amounts of heavy impurity strongly influence the dielectric properties of the solidified inert gases. The data of Amey and Cole, corrected to 5461 Å using the dispersion information from the present investigation and a graphical extrapolation, yield dielectric constants equivalent to $n=1.346$ and $n=1.298$ for the solid and liquid at the triple point (cf. 1.3462 and 1.3032). Smoothed values for the refractive indices, and the f_{LL} functions of liquid and solid krypton for 5461 Å are given in Table II. The behavior of these functions is discussed in Sec. V. The gas was supplied by the British Oxygen Company and was stated to be 99.99% pure, the principal impurities being xenon (~0.005%) and nitrogen (~0.003%).

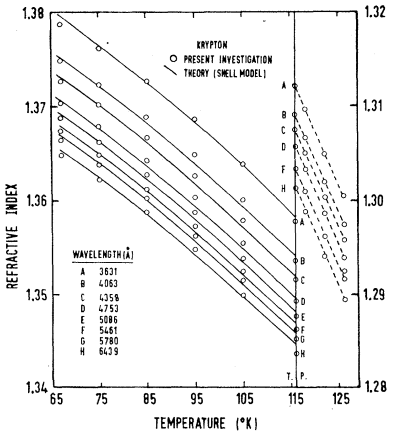

FIG. 4. Refractive indices of liquid and solid krypton. The continuous lines correspond to Eq. (12) with values $\omega_0 = 10.03$ eV, $\omega_p^2 = 29.10$ eV², $\mathcal{U}_0^3(\mathrm{TP}) = 7.55$ eV², $\chi_1 = 0.3578$, and $B_3 = 12$. To avoid confusion, not all data points are included in the figure.

[30] E. H. C. Parker, H. R. Glyde, and B. L. Smith, Phys. Rev. **176**, 1107 (1968).
[31] H. R. Glyde, J. Phys. Chem. Solids **27**, 1659 (1966).
[32] B. L. Smith, Phil. Mag. **6**, 939 (1961).
[33] G. O. Jones and J. M. Woodfine, Proc. Phys. Soc. (London) **86**, 101 (1965).

TABLE III. Smoothed values of refractive index, density, and f_{LL} for liquid and solid xenon as a function of wavelength (Å). f_{LL} is computed for 5461 Å, using bulk density values for the solid.

T °K	Wavelength (Å) 6439	5780	5461	5086	4806	4700	4358	4063[b]	3650[b]	3612[b]	ρ[a] (10^{-2} mole/ cm³)	LL cm³/mole
Solid												
80	1.4808	1.4833	1.4854	1.4882	1.4906	1.4917	1.4954	1.4995	1.5080	1.5091	2.771	10.350
90	1.4775	1.4800	1.4821	1.4848	1.4873	1.4884	1.4921	1.4962	1.5047	1.5058	2.750	10.365
100	1.4740	1.4765	1.4786	1.4814	1.4838	1.4849	1.4886	1.4927	1.5012	1.5024	2.730	10.380
110	1.4701	1.4727	1.4748	1.4775	1.4800	1.4811	1.4848	1.4889	1.4974	1.4986	2.709	10.388
120	1.4660	1.4686	1.4706	1.4734	1.4759	1.4770	1.4807	1.4848	1.4934	1.4945	2.687	10.396
130	1.4616	1.4641	1.4662	1.4690	1.4715	1.4726	1.4763	1.4804	1.4890	1.4901	2.664	10.399
140	1.4569	1.4594	1.4616	1.4643	1.4668	1.4679	1.4716	1.4757	1.4843	1.4855	2.640	10.403
150	1.4520	1.4545	1.4566	1.4594	1.4619	1.4629	1.4667	1.4708	1.4794	1.4805	2.615	10.407
161.35	1.4461	1.4486	1.4507	1.4535	1.4560	1.4571	1.4608	1.4650	1.4736	1.4747	2.585	10.411
Liquid												
161.35	1.3876	1.3900	1.3918	1.3937	1.3957	1.3967	1.4001	1.4041	1.4103	1.4111	2.272	10.475
166	1.3830	1.3853	1.3871	1.3891	1.3911	1.3921	1.3955	1.3995	1.4057	1.4065	2.244	10.494
170	1.3790	1.3814	1.3832	1.3851	1.3872	1.3882	1.3916	1.3956	1.4017	1.4025	2.221	10.507
174	1.3748	1.3772	1.3790	1.3809	1.3830	1.3840	1.3874	1.3914	1.3976	1.3984	2.198	10.513
178	1.3708	1.3732	1.3750	1.3770	1.3790	1.3800	1.3834	1.3874	1.3936	1.3944	2.176	10.520

[a] Solid densities, A. J. Eatwell and B. L. Smith, Phil. Mag. **6**, 461 (1961); J. R. Packard and C. A. Swenson, J. Phys. Chem. Solids **24**, 1405 (1963): liquid densities, A. J. Leadbetter and H. E. Thomas, Trans. Faraday Soc. **61**, 10 (1965).
[b] Values deduced from photographs.

C. Liquid and Solid Xenon

The refractive indices of liquid and solid xenon are shown in Fig. 5. Fluid xenon has been studied extensively[27,34] in the density range 0–20 millimoles cm^{-3}, and values of refractive index extrapolated to the triple point (22.7 millimoles cm^{-3}) give agreement to within 0.0004 of the present results. The dielectric-constant data of Amey and Cole yield values equivalent to $n=1.443$ and $n=1.385$ (5461 Å) for the solid and liquid at the triple point (cf. 1.451 and 1.392, respectively). Smoothed values for the refractive indices and f_{LL} functions of liquid and solid xenon for 5461 Å are given in Table III. The behavior of these functions is discussed in Sec. V.

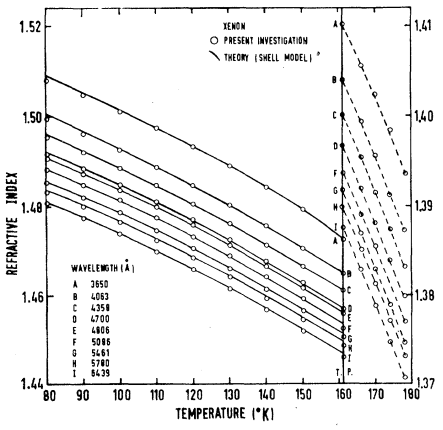

FIG. 5. Refractive indices of liquid and solid zenon. The continuous lines correspond to Eq. (12) with values $\omega_0=8.43$ eV, $\omega_p^2=23.145$ eV^2, $\mathcal{U}_0^3(\mathrm{TP})=3.35$ eV^2, $\chi_1=0.47425$, and $B_3=12$. To avoid confusion, not all data points are included in the figure.

[34] D. H. Garside, H. V. Mølgaard, and B. L. Smith, J. Phys. **B1**, 449 (1968).

The xenon gas was supplied by the British Oxygen Company and was stated to be 99.99% pure, the principal impurities being 0.005% nitrogen and 0.0025% krypton. Two different cylinders of gas were used with indistinguishable results.

V. DISCUSSION OF RESULTS

De Boer and Blaisse[35] have shown that the solidified inert gases obey a quantum-mechanical law of corresponding states, which may be stated as

$$p^*=p^*(V^*,T^*,\lambda) \tag{3}$$

where $p^*=p\sigma^3/\epsilon'$, $V^*=V/N\sigma^3$, $T^*=kT/\epsilon'$, and $\lambda=h/[\sigma(2m\epsilon')^{1/2}]$. λ is a measure of the importance of quantum effects, and the parameters σ and ϵ' are the characteristic length and energy associated with each substance, appearing in the two-body interaction potential $\phi(r)=\epsilon' f(r/\sigma)$.

Bernardes[36] obtained power series in λ for properties at $T=0$°K. The result for the molar volume is

$$V_0^*(\lambda)=V_0^*(0)(1+2.02\lambda+5\lambda^2), \tag{4}$$

where $V_0^*(\lambda)=V_0/N\sigma^3$, and $V_0^*(0)=0.916$ is the limiting value of the reduced volume as $\lambda\rightarrow 0$. If, at sufficiently high temperatures, quantum effects become negligible, then

$$V_T^*(\lambda)\approx V_T^*(0)=V_T/N\sigma^3. \tag{5}$$

From (4) and (5), the molar density $\rho=1/V$ may therefore be expressed as

$$\rho_T^*(\lambda)=\rho_T\rho_0^*(\lambda)/\rho_0, \tag{6}$$

[35] J. de Boer and B. S. Blaisse, Physica **14**, 149 (1948).
[36] N. Bernardes, Phys. Rev. **120**, 807 (1960).

and thus the Lorentz-Lorenz function becomes

$$f_{LL,T}^*(\lambda)=f_{LL,T}f_{LL,0}^*(\lambda)/f_{LL,0}. \quad (7)$$

Values of the reduced Lorentz-Lorenz functions for solid argon, krypton, and xenon normalized at $\rho_T^*(\lambda)=0.98$ and based on the parameters given in Table IV are shown in Fig. 6. At reduced densities below $\rho_T(\lambda)=0.98$, a slight positive slope is observed for krypton. As discussed in Sec. III A, the results for argon may be interpreted so as to behave in a similar way. However, it is thought that the effect is spurious and arises because of the difficulty in accurately matching dielectric constant and density data close to the triple point. In the case of krypton the rise could be removed by reinterpreting the existing density data by postulating a vacancy concentration of $\sim 0.1\%$ at the triple point.

At lower densities all three substances show an accelerated change in $f_{LL,T}^*(\lambda)$ with increasing density. One might expect from a rough estimate of the expected overlap that the rate of decrease is likely to be greatest in argon and least in xenon, with krypton intermediate in behavior. The more rapid decrease in $f_{LL,T}^*(\lambda)$ shown for krypton in Fig 6 might be due to experimental error either in the density or the refractive index and may therefore not be significant. It is interesting to note, however, that a similar juxtaposition has been observed for other properties of the solidified inert gases, such as isothermal compressibility.[37]

Normalization could, of course, be carried out in terms of T^*, instead of reduced density. Alternatively, Eq. (5) could be used directly without quantum corrections, by using appropriate values of σ.[38] We have carried out both procedures with results that are qualitatively similar to those outlined above.

In the case of the liquids, an analysis using the law of corresponding states has been carried out by reducing f_{LL} and density to values at the critical point[39] (Fig. 7). The density data available for the low-temperature liquids are somewhat sparse and may well be unreliable, particularly for krypton. We thus consider that the curves for argon and xenon represent the true behavior of f_{LL} of the liquids in this region, in agreement with observations made on the liquids at lower densities,[26,34] and that the apparent behavior of krypton is probably spurious.

TABLE IV. Parameters used to reduce solid densities for law of corresponding states analysis.

	ρ_0 (mole/cm³)	λ	$\rho_0^*(\lambda)/\rho_0$	$f_{LL,0}^*(\lambda)/f_{LL,0}$
Argon	0.044342	0.0212	2.3559	0.42448
Krypton	0.036897	0.0113	2.8909	0.34591
Xenon	0.028812	0.0070	3.7355	0.26770

[37] A. O. Urvas, D. L. Losee, and R. O. Simmons, J. Phys. Chem. Solids **28**, 2269 (1967).

[38] G. K. Horton and J. W. Leech, Proc. Phys. Soc. (London) **82**, 816 (1963).

[39] E. A. Guggenheim, J. Chem. Phys. **13**, 253 (1945).

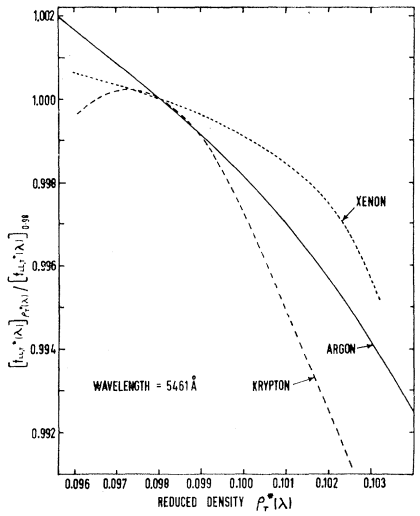

FIG. 6. Variation of the reduced functions f_{LL} of solid argon, krypton, and xenon with reduced density for 5461 Å. The curves are normalized at $\rho_T^*(\lambda)=0.98$ and based on the parameters given in Table IV.

VI. COMPARISON WITH THEORY

The absorption spectra of solid argon, krypton, and xenon have recently been studied.[40] In each case, doublets have been observed close to the atomic resonance doublets. These may be interpreted in terms of Wannier excitons[41] with $r=1$, built from a spin-orbit split valence band and the lowest conduction band. In addition, extra lines are observed at higher energies that are found to fit a Wannier series with $r=2, 3, \cdots$ at $\mathbf{k}=0$ (Γ point) in the Brillouin zone. For such a series, the binding energy G is related to the energy gap E_G between the higher valence band and the con-

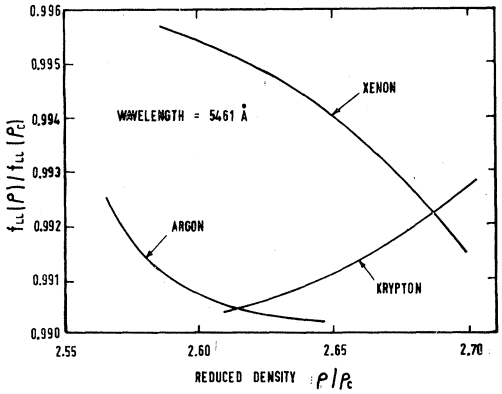

FIG. 7. Variation of the reduced functions f_{LL} of liquid argon, krypton, and xenon with reduced density for 5461 Å. The curves are normalized to estimated f_{LL} and ρ values at the critical point.

G. Baldini, Phys. Rev. **128**, 1562 (1962); O. Schnepp and K. Dressler, J. Chem. Phys. **33**, 49 (1960); O. Bostanjoglo and L. Schmidt, Phys. Letters **22**, 130 (1966); I. T. Steinberger and O. Schnepp, Solid State Commun. **5**, 417 (1967); D. Beaglehole, Phys. Rev. Letters **15**, 551 (1965).

[41] R. J. Elliott, Phys. Rev. **108**, 1384 (1957); R. S. Knox (private communication).

TABLE VI. Calculation and comparison with experiment of polarizability change from gas to solid for two-level tight-binding exciton model (Ref. 3). Values for r_0, ϵ', and σ were taken from Ref. 38; gas data from Refs. 28 and 44.

	r_0 (Å)	$\epsilon'(10^{-16}$ erg)	σ (Å)	ΔE(eV)	E_0(eV)	$\Delta E/E_0$ (%)	Expt. % (n)	Expt. % (ϵ)
Argon	3.87	165	3.402	0.137	11.725	1.31±0.15	1.05	0.85
Krypton	4.04	227	3.637	0.218	10.03	2.17±0.23	1.29	0.64
Xenon	4.46	320	3.936	0.273	8.43	3.50±0.7	0.70	2.00

duction band by the hydrogenlike relation

$$h\nu_r = E_G - G/r^2 \quad r=1, 2, 3, \cdots, \tag{8}$$

where $G=\mu\epsilon^{-2}$ Ry, ϵ is the dielectric constant, and μ is the reduced mass of the exciton in electron mass units, given by

$$\mu^{-1} = m_e^{*-1} + m_h^{*-1}. \tag{9}$$

Since the radii are given by $a_r = \epsilon\mu^{-1}r^2$ Bohr radii, these may be estimated by combining values of $\epsilon(=n^2)$ obtained in the present investigation with values of G extracted from the uv absorption spectra. Values for $a_r=1$ computed from Eq. (8) and given in Table V are seen to be only slightly greater than the interatomic spacings, whereas a_2, a_3, $\cdots$ are considerably greater. Thus, the $r=1$ excitons are intermediate in radius and could be considered tightly bound. Data for the polarizability and uv dispersion of argon, for example, indicate[5] that the number of electrons that contribute to the dielectric properties is $N\approx 8.7$. Since the ground-state configuration of argon is $KL3s^23p^6$, this suggests that only the outer electrons contribute significantly, and thus a tight-binding model based on lowest-energy level transitions only might be expected to describe the dielectric properties to a reasonable approximation. Such a model has been quite successful[36] when applied to the electronically similar alkali halides.

Mazo[3] has carried out a computation using second quantization and thermodynamic Green's functions and has obtained the Lorentz-Lorenz functions for the solids by estimating the difference Δf_{LL} between a low-pressure gas and a solid for a two-level (ground and one-excited state), tight-binding model. The result for the solid is

$$f_{LL} = (1-2f)\tfrac{4}{3}\pi\alpha \tag{10}$$

where f is the probability that a given atom is in the true many-body ground state of the system (E_0), which may be evaluated for a fcc lattice[42] since

$$2f/(1-2f)^3 = \Delta E/E_0 = 28.908(\epsilon'/E_0)(\sigma/r_0)^6, \tag{11}$$

where ϵ' and σ are the Lennard-Jones parameters defined by $\phi(r)=4\epsilon'[(\sigma/r_0)^m-(\sigma/r_0)^6]$, and ΔE represents the attractive part of the binding energy of the crystal. Experimental data from the present investigation and dielectric constant values from Amey and Cole are compared with Δf_{LL} evaluated from Eq. (11) in Table VI.

Agreement is reasonable for argon, but the experimental values of Δf_{LL} for krypton and xenon are inconsistent. This might be due to inaccuracies in the gas data. The uncertainty in accurately matching dielectric constant and density data for the solids near the triple point will also contribute significantly to the possible error.

It should be noted that the computed values of $\Delta E/E_0$ are strongly dependent on the values of ϵ' and σ chosen. For example, if values corresponding to $m=12$ and all neighbors are used for xenon, then $\Delta E/E_0 = 2.55\%$, whereas if nearest-neighbor-only parameters are used, then $\Delta E/E_0 = 3.91\%$. The error limits in Table VI indicate the possible range covered by using nearest-neighbor, or all neighbor, parameters given by Horton and Leech[38] for $m=10$–14.

A second tight-binding approach is due to Doniach and Huggins, who have described the dielectric properties of the solids by a semiphenomenological shell model, in which the atoms are represented by localized electron oscillators and are coupled via dipole-dipole and nearest-neighbor forces. This is similar to the Dick-

TABLE V. Exciton radius a_1 calculated for solid argon, krypton, and xenon from Eq. (8) using the present refractive-index data extrapolated to zero frequency. The atomic separation is assumed to be half the appropriate interatomic spacing in the lattice.

	Temp. (°K)	n_0^2	G (eV)	μ (electron mass)	a_1 (Bohr radii)	Atomic sep. (Bohr radii)
Argon[a]	20	1.660	2.1	0.43	3.91	3.55[b]
Krypton[a]	20	1.882	1.73	0.45	4.18	3.78[c]
Xenon[a]	4.2	2.217	1.08	0.39	5.69	4.11[d]

[a] See Ref. 40.
[b] See Ref. 29.
[c] B. F. Figgins and B. L. Smith, Phil. Mag. 5, 186 (1960).
[d] A. J. Eatwell and B. L. Smith, Phil. Mag. 6, 461 (1961); J. R. Packard and C. A. Swenson, J. Phys. Chem. Solids 24, 1405 (1963).

TABLE VII. Shell-model parameters extracted from experimental data for solid argon, krypton, and xenon (Ref. 2).

	ω_0 (eV)	ω_p^2 (eV^2)	V_0^3(TP) (eV^2)	B_3	χ_1
Argon	11.725	31.69	7.99	12	0.2811
	17.6	157.57	6.21	14.43	0.0
Krypton	10.03	29.10	7.55	12	0.35780
	15.0	146.893	9.91	8.33	0.0
Xenon	8.43	23.145	3.35	12	0.47425
	12.75	130.305	3.70	11.34	0.0

[42] J. O. Hirschfelder, C. F. Curtiss, and R. B. Bird, *Molecular Theory of Gases and Liquids* (Wiley-Interscience, Inc., New York, 1954) p. 1040.

Overhauser[43] model which has been successfully applied to the alkali halides,[44] for example, by Cowley[45] and by Mistkevich.[46] The dielectric properties are assumed to result mainly from the lowest level uv band ($^3P_1 \rightarrow {}^1S_0$ transition), which is represented by a single density-dependent Frenkel exciton line.

The Lorentz-Lorenz function is given by

$$3\frac{(n^2-1)}{(n^2+2)}\frac{1}{\rho}=\frac{\omega_p^2}{\omega_0^2+\mathcal{U}_0^3(T)-\omega^2}+\chi_1=\chi_0+\chi_1, \quad (12)$$

where ω_p^2 represents the dipole-dipole interaction of the lowest atomic states, ω_0 is the natural frequency of the noninteracting atomic oscillators ($\omega_0 \gg \omega$), and $\mathcal{U}_0^3$ corresponds to the shift in ω_0^2 observed with increasing density and produced by the shell-core forces. The term χ_1, assumed to be frequency-independent, was introduced to take account of the core polarizability and possible contributions to the exchange integrals from higher atomic states.

We have fitted the present data to Eq. (12) as follows: A value of $\mathcal{U}_0^3$ was chosen at the triple point and evaluated for other temperatures by assuming that

$$\mathcal{U}_0^3(T)=\mathcal{U}_0^3(\mathrm{TP})\exp[-B_3(a_T-a_{\mathrm{TP}})/a_0], \quad (13)$$

where a_0, a_{TP}, and a_T are the appropriate lattice parameters. The density ρ was normalized to ρ_{TP} for convenience. The constant B_3 was given integer values in the range 4–16.

In the case of argon, ω_0 was set equal to the mean of the spin-orbit-split lowest uv absorption frequencies for the gas ($^1S_0$-$^3,^1P_1$ spin-orbit doublet). For krypton and xenon, however, the splitting is relatively greater (argon $\Delta E/E \approx 1.8\%$, krypton $\approx 5.1\%$, xenon $\approx 12.7\%$), and ω_0 was set equal to the lower-energy value (Table VII).

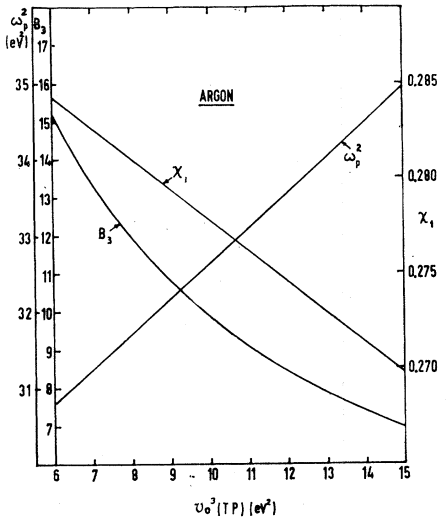

FIG. 8. Variation of the short-range exponent B_3, the plasma frequency ω_p^2, and contribution from higher excited states χ_1, with $\mathcal{U}_0^3$(TP) for solid argon.

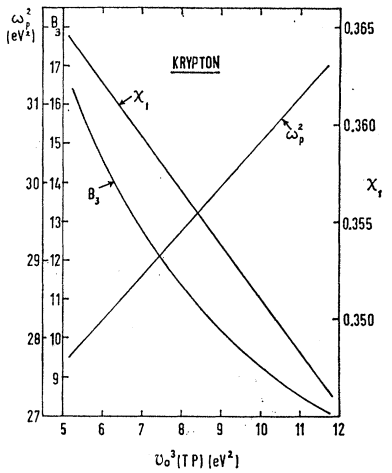

FIG. 9. Variation of the short-range exponent B_3, the plasma frequency ω_p^2, and contribution from higher excited states χ_1, with $\mathcal{U}_0^3$(TP) for solid krypton.

For each B_3, a least-squares fit of the experimental data given in Tables I–III was made to Eq. (12) to extract values for ω_p^2 and χ_1, the procedure being repeated for other values of $\mathcal{U}_0^3$(TP). It was found possible to obtain ω_p^2 and χ_1 for each $\mathcal{U}_0^3$(TP) such that χ_1 was independent of density within experimental error. The parameters B_3, ω_p^2, and χ_1 thus derived were plotted as a function of $\mathcal{U}_0^3$(TP) (Figs. 8–10). Since one would expect that $B_3 \approx m$, where $4\epsilon'(\sigma/r_0)^m$ is a short-range force of the Lennard-Jones type, values of ω_p^2, χ_1, and $\mathcal{U}_0^3$(TP) corresponding to $B_3=12$ were taken from the graphs and used to compute the temperature and wave-

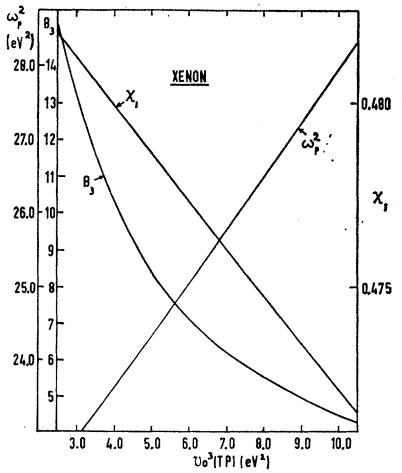

FIG. 10. Variation of the short-range exponent B_3, the plasma frequency ω_p^2, and contribution from higher excited states χ_1, with $\mathcal{U}_0^3$(TP) for solid xenon.

[43] B. G. Dick and A. W. Overhauser, Phys. Rev. **112**, 90 (1958).
[44] M. Born and K. Huang, in *Dynamical Theory of Crystal Lattices* (Oxford University Press, Oxford, 1954), Sec. 9.
[45] R. A. Cowley, W. Cockran, B. N. Brockhouse, and A. D. B. Woods, Phys. Rev. **131**, 1030 (1963).
[46] V. V. Mitskevich, Fiz. Tverd. Tela **3**, 3036 (1961) [English transl.: Soviet Phys.—Solid State **3**, 2211 (1962)].

length dependence of the refractive indices. (See Table VII and Figs. 2, 4, and 5.)

The terms χ_0 and χ_1 in Eq. (12) contribute approximately equal amounts to the molar polarizability. In view of the somewhat arbitrary form of Eq. (12) and choice of ω_0, the fitting procedure was repeated to determine whether (a) the fit could be improved by altering ω_0, (b) the fit would significantly worsen if $\chi_1=0$ and ω_0 were allowed to change its value, and (c) the parameters extracted depend on the frequency range of the data used to obtain the fit.

For each solid it was found that the standard deviation of the fit was improved by a few percent by assigning a higher energy value to ω_0. For example, by putting $\omega_0=9.6$ eV for xenon, $V_0^3(\mathrm{TP})\approx 2$ eV^2, $\omega_p^2=38.7$ eV^2 $\chi_1=0.373$, and the standard deviation is reduced by 5%. The effect of (b) is summarized in Table VII. Restricting χ_1 to zero is equivalent to regarding the atom as a single oscillator, and results in the fit becoming slightly worse. For each solid, ω_0 is shifted to higher energy and ω_p^2 is increased considerably. Varying the frequency range was found to change the parameters only slightly. For example, by reducing the data to the optical region only (60% of total data), $V_0^3(\mathrm{TP})$ decreases by ~8%, χ_1 decreases by ~2%, and ω_p^2 increases by ~1–2% for all substances, argon being affected most and xenon least.

In view of the slight uncertainty in the slope of the Lorentz-Lorenz functions of argon and krypton near their triple points (see Sec. V), the effect of only including data in the above analysis from that part of the curve for which the Lorentz-Lorenz function decreases unambiguously with increasing density was also examined. This procedure gave a slightly higher value of $V_0^3(\mathrm{TP})$ (extrapolated), but ω_p^2 and χ_1 remained essentially unchanged. Doniach and Huggins obtained

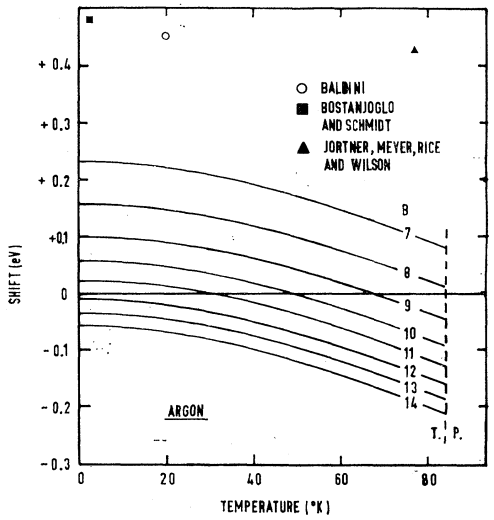

FIG. 11. Comparison of theoretical uv shift (exciton frequency) predicted from Eq. (14) with experiment for solid argon.

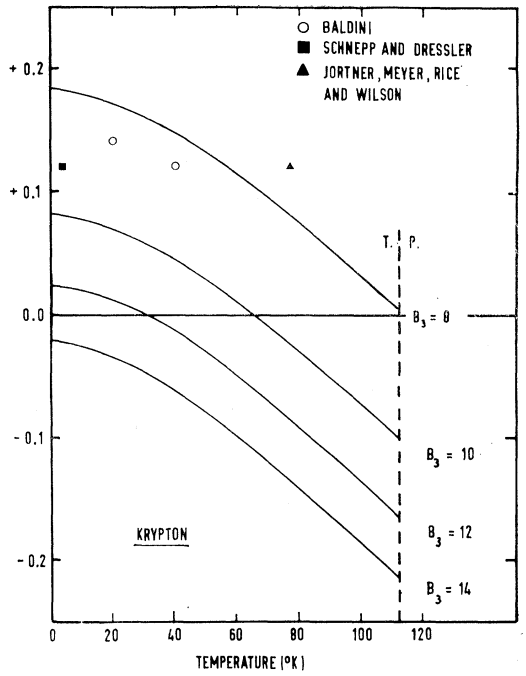

FIG. 12. Comparison of theoretical uv shift (exciton frequency) predicted from Eq. (14) with experiment for solid krypton.

$V_0^3(\mathrm{TP})=10$ eV, $\omega_p^2=35$ eV^2, and $\chi_1=0.28$ for solid argon from much more limited experimental data (50–70°K).

As a check of the model, an attempt was made to predict the shift of the lowest uv peaks in the solids from the gas values, by determining the exciton frequencies ω_{ex}. Assuming that χ_1 is indeed independent of frequency,

$$\omega_{ex}^2=\omega_0^2+V_0^3(\mathrm{TP})-\frac{\omega_p^2}{q}\left(\frac{2\chi_1+3}{3-\chi_1}+2\right). \quad (14)$$

Since appropriate values of ω_p^2 and χ_1 have already been obtained for each choice of $V_0^3(\mathrm{TP})$ by the above fitting procedure, these may be used together with an assumed value for B_3 to extrapolate to the temperatures at which Baldini and others made their experimental observations of the absorption spectra (Figs. 11–13). From the figures, it appears that $B_3\approx 6$–8, which is significantly lower than the value $B\approx 12$ required by the short-range hypothesis. The difference might be due to experimental error, since there is some disagreement between shifts reported by different observers. It is more likely, however, that it is unreasonable to use the shell model in a region of strong absorption as a means of establishing values for B_3.

A third tight-binding approach is due to Keil,[1] who has calculated the static polarizability α of an argon atom in the solid, by estimating the contribution to α of each electron shell by means of a linear variational technique. The calculation confirms that about 95% of the total polarizability is due to the $3p^6$ electrons, and

most of the density dependence is due to variations in this contribution, as implied by the tight-binding model. The results are expressed as a variation of the reduced polarizability α_T/α_∞ with reduced lattice parameters a_T/a_0, where α_∞ is the polarizability of the free atom at infinite attenuation, and a_T and a_0 are the lattice parameters at T°K and 0°K. Assuming that the molar polarizability of the free atom[47] is 4.222 cm^3 mole^{-1} at 5461 Å, comparison with the present data suggests that at 78°K the polarizability decreases by ~1.5% compared with ~3.5% predicted by theory. In view of the difficulties noted by Keil in evaluating α_∞ theoretically, a more realistic comparison may be made with experiment by examining values for the rate of change of the reduced Lorentz-Lorenz function with the reduced lattice parameter $d(f_{LL}{}^R)/d(a^R)$ at temperatures in the range studied. This may be carried out numerically, or graphically as in Fig. 3, in which theoretical values have been normalized such that they coincide with the results of the present investigation at $\rho/\rho_0=0.96$. Agreement is better at lower temperatures than near the triple point. At 78°K, the slope of the experimental curve is ~0.2 compared with a theoretical slope of ~0.5. The slope $d(f_{LL}{}^R)d(a^R)$ for the pressure dependence of the refractive index was estimated by Smith and Pings[48] to be 0.47±0.04 at 78°K. It would be interesting to determine what effect a consideration of overlap and exchange would have on the theoretical result.

VII. CONCLUSION

We conclude that the Lorentz-Lorenz functions of the inert gases remain constant to within a few percent over the entire density range from the low-pressure gas to the solid. Comparison of the present data with previous results for argon and zenon at lower densities suggests that the total variation in the fluid, including the critical region, may be smaller than ~1.5%, and that a small decrease in f_{LL} (~1%) occurs on freezing. This may be due to the high symmetry of the crystal lattice in which, unlike the liquid, contributions from configurational terms to the polarizability are negligible.

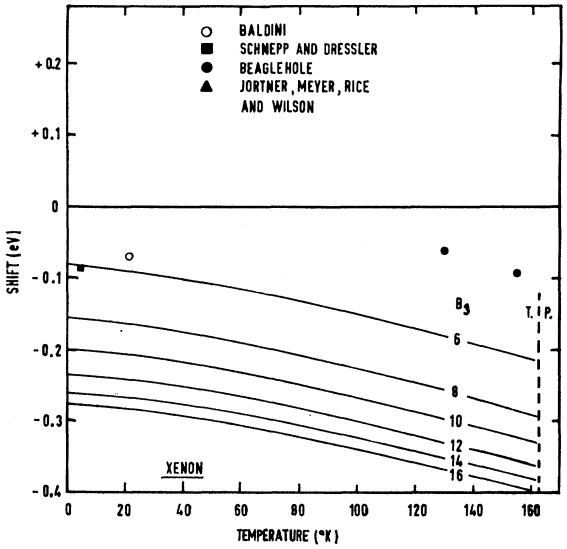

FIG. 13. Comparison of theoretical uv shift (exciton frequency) predicted from Eq. (14) with experiment for solid xenon.

There is some doubt as to the behavior of the Lorentz-Lorenz functions of the solids near their triple points, possibly due to annealing and other nonequilibrium processes taking place. At higher densities however the Lorentz-Lorenz functions decrease unambiguously with increasing density at an accelerating rate, presumably due to the increasing effect of overlap on the exchange integrals. The rate of decrease is in rough agreement with calculations by ten Seldam and de Groot[14] based on the Thomas-Fermi atom, in which the boundary conditions are varied in order to take into account the decreasing effective atomic radius.

Comparison of the experimental results with calculations based on tight-binding exciton models are encouraging, but refinement of the refractive-index data and more accurate density measurements are necessary before a definitive test of these theories may be made. At present the behavior of the Lorentz-Lorenz function for solid krypton appears to be inconsistent compared with that of argon and xenon.

[47] C. Cuthbertson and M. Cuthbertson, Proc. Roy. Soc. (London) **A84**, 13 (1910); D. R. Johnston, G. J. Oudemans, and R. H. Cole, J. Chem. Phys. **33**, 1310 (1960).

[48] B. L. Smith and C. J. Pings, J. Chem. Phys. 48, 2387 (1968).